Connectivity Scaling Laws in Wireless Networks

Justin P. Coon, Orestis Georgiou, and Carl P. Dettmann

***Abstract*—We present scaling laws that dictate both local and global connectivity properties of bounded wireless networks. These laws are defined with respect to the key system parameters of per-node transmit power and the number of antennas exploited for diversity coding and/or beamforming at each node. We demonstrate that the local probability of connectivity scales like $O(z^{\mathcal{C}})$ in these parameters, where $\mathcal{C}$ is the ratio of the dimension of the network domain to the path loss exponent, which we term the *connectivity exponent*. Our results point to an underlying universality property of wireless networks, which can be useful in characterizing network performance.**

***Index Terms*—Networks, connectivity, boundaries, MIMO.**

I. Introduction

Ad hoc wireless networks have found use in applications ranging from environmental monitoring to vehicle-to-vehicle communication. These networks possess commonality insomuch as the number and distribution of nodes in the network is often random. Fundamentally, it is of great interest to be able to determine the probability that such a network is *fully* connected [1], [2]. This understanding can lead to improved protocols and network deployment strategies in practice [3].

For dense networks, several analytical results on connectivity have been published (see, e.g., [4]), particularly in the form of insightful scaling laws. For example, in [5], the authors derive a power scaling law that ensures full connectivity is achieved *almost surely* as the number of nodes in the network tends to infinity. In [6], the number of nearest neighbors required to achieve full connectivity asymptotically is studied. Related results are given in [7] for sectorized networks.

While early works considered unbounded networks, more recent research has attempted to better quantify the role that boundaries play in network analysis. Simple confining geometries (e.g., cubes, spheres) were studied in [2], [4], [8], [9]. Networks with nodes confined to a square lattice were addressed in [10]. A more versatile framework based on a cluster expansion approach was recently detailed in [11]. This theory is capable of treating more complicated geometrical network domains and encompasses several aspects of subsequently reported theories (cf. [2], [9]). The framework has also been shown to yield more accurate results than conventionally accepted approximations in some cases [2].

In this paper, we adopt the theory detailed in [11] to derive new scaling laws that describe both local and global connectivity properties of bounded random geometric networks. These laws are defined with respect to two system parameters: the per-node transmit power and the number of antennas employed by each device. Our results are twofold. First, we show that the local (pairwise) probability of connectivity scales like $O(z^{\mathcal{C}})$ in terms of both system parameters, where $\mathcal{C}$ is the ratio of the dimension of the network domain to the path loss exponent. Second, we investigate two multi-antenna transmission schemes – orthogonal space-time block coding (STBC) and beamforming (multiple-input, multiple-output with maximum ratio combining - MIMO-MRC) – and analyze their relative merits with respect to antenna scaling. This contribution marks the first time such a comparison has been made, particularly in reference to global network performance.

J. P. Coon is with the Department of Engineering Science, University of Oxford, Parks Road, Oxford, UK, OX1 3PJ; tel: +44 (0)1865 283 393, (e-mail: justin.coon@eng.ox.ac.uk).

O. Georgiou is with the Toshiba Telecommunications Research Laboratory, 32 Queen Square, Bristol, UK, BS1 4ND.

C. P. Dettmann is with the School of Mathematics, University of Bristol, University Walk, Bristol, UK, BS8 1TW.

II. Network Model and Background Theory

Consider a network of N uniformly distributed nodes with locations $\mathbf{r}_i \in \mathcal{V} \subseteq \mathbb{R}^d$ for $i = 1, 2, \ldots, N$. The node density is $\rho = N/V$, where $V = |\mathcal{V}|$ and $|\cdot|$ denotes the size of the set. Here, we use the Lebesgue measure of the appropriate dimension d. Any two nodes i and j a distance $D(\mathbf{r}_i, \mathbf{r}_j)$ apart are directly connected with probability $H(D(\mathbf{r}_i, \mathbf{r}_j))$, which we write as $H(\mathbf{r}_{ij})$ or H_{ij}.

We are interested in observing network connectivity at high node density, for which the full connectivity probability, averaged over all possible node configurations in $\mathcal{V}$, is [11]

$$P_{fc} \approx 1 - \rho \int_{\mathcal{V}} e^{-\rho \int_{\mathcal{V}} H(\mathbf{r}_{12}) \mathrm{d}\mathbf{r}_1} (1 + O(N^{-1})) \mathrm{d}\mathbf{r}_2. \quad (1)$$

For the approximation given in (1), we require that P_{fc} is high, i.e., the smallest expected degree is large.

Taking a closer look at the integral in the exponent in (1), which we denote by the functional

$$M[H; \mathbf{r}_2] = \int_{\mathcal{V}} H(\mathbf{r}_{12}) \, \mathrm{d}\mathbf{r}_1 \quad (2)$$

we see that it defines the likelihood that a node located at $\mathbf{r}_2$ will connect to some other arbitrary node in the network domain. In previous work, this functional has been linked to key network observables, such as the pair formation probability, the mean degree, and the minimum network degree, each increasing monotonically with M [12]. Due to its importance and its physical meaning, we call M the *connectivity mass*.

The relationship between M and P_{fc} is clear from (1): as M increases, the probability that the network is connected increases. In the dense regime, we can observe this behavior explicitly to leading order by expanding M at $\mathbf{r}_2$ situated on a boundary, which yields the leading-order expression [11]

$$M \approx \omega \int_0^{\infty} r^{d-1} H(r) \, \mathrm{d}r \quad (3)$$

where $\omega = \int \mathrm{d}\Omega$ is the solid angle as seen from $\mathbf{r}_2$, with $\Omega = 2\pi^{d/2}/\Gamma(d/2)$ being the full solid angle in d dimensions.

Due to its direct link to P_{fc}, the connectivity mass, as defined in (3), will be used to develop scaling laws in certain parameters below. Although presented in a leading-order form here, this form exactly dictates the global network connectivity probability.

III. Scaling Laws

Here, we exploit the connectivity mass M (see (3)[1]) to develop local (pairwise) connectivity scaling laws with respect to the per-node transmit power and number of antennas exploited by each device in the network.

A. Transmit Power

To study the scaling behavior with respect to the per-node transmit power P_T (equivalently, the average received SNR), we must define the pairwise connection function H. For the sake of generality, we adopt a definition related to the SNR outage probability, such that H_{ij} is the probability that the SNR at the destination node exceeds a threshold SNR_{th}, i.e.,

$$H_{ij}(r) = P(\mathsf{SNR}(r) \cdot X_{ij} > \mathsf{SNR}_{th}) \tag{4}$$

where X_{ij} denotes the random variable signifying the gain of the channel between nodes i and j and $\mathsf{SNR} \propto P_T$ is the average received SNR, which is a function of the distance r between the nodes in question. Other definitions can be adopted for H_{ij}, including the complement of the mutual information outage probability[2]. Often, such definitions can often be expressed as the (complementary) cumulative distribution function (CDF) of X_{ij} as shown above.

For isotropically radiating nodes, the Friis transmission formula stipulates that $\mathsf{SNR} \propto r^{-\eta}$ where η is the pass loss exponent. Typically, $\eta = 2$ if propagation occurs in free space, with $\eta > 2$ in cellular/cluttered environments. Consequently,

$$H_{ij}(r) = 1 - F_{X_{ij}}(\beta r^{\eta}) \tag{5}$$

where $F_{X_{ij}}$ is the CDF of X_{ij} and $\beta \propto P_T^{-1}$ depends on the center frequency of the transmission and the power of the noise process at the receiver (β defines the length scale).

To derive the local scaling law with respect to P_T, we begin with (3). Substituting for H (and omitting i and j) yields

$$\begin{aligned} M &= \omega \int_0^{\infty} r^{d-1}(1 - F_X(\beta r^{\eta}))\,\mathrm{d}r \\ &= \frac{\omega}{\beta^{\mathcal{C}}\eta} \int_0^{\infty} x^{\mathcal{C}-1}(1 - F_X(x))\,\mathrm{d}x \end{aligned} \tag{6}$$

where we define

$$\mathcal{C} = \frac{d}{\eta} \tag{7}$$

to be the *connectivity exponent*. Under the assumption that $\mathbb{E}[X^{\mathcal{C}}] < \infty$, with $\mathbb{E}[\cdot]$ denoting the expectation operator, the integral in (6) is bounded, and it follows that we can write

$$M = K_1 P_T^{\mathcal{C}} \tag{8}$$

where K_1 is a constant independent of P_T.

The power law given above provides useful insight into the behavior of random geometric networks, which can be used to enhance network designs in practice. It is particularly interesting to note the conditions under which power scaling provides a progressive improvement to local connectivity, versus those conditions under which diminishing returns are experienced with an increase in P_T. For example, a high-dimensional network (e.g., $d = 3$) operating in low path loss conditions will benefit from the former behavior as P_T is increased; however, a low-dimensional network located in a cluttered environment where high path loss conditions prevail will experience the latter. The critical transition point is $\mathcal{C} = 1$.

We conclude this discussion by pointing out that the power law (8) arises from the fact that $M \propto \beta^{-\mathcal{C}}$. Thus, one can infer that scaling laws in other key system parameters are affected by the connectivity exponent in the same way (e.g., carrier frequency/wavelength and antenna gain). This conclusion follows directly from the Friis transmission formula.

B. Multi-Antenna Systems

Consider the case where each node in the network possess m transmit antennas and n receive antennas, and one of two signalling mechanisms is employed: diversity coding following the conventional STBC scheme derived from generalized complex orthogonal designs (GCODs) [14], and transmitter/receiver beamforming, also known as MIMO-MRC [15].

1) Diversity Coding: It is well known that the performance of a point-to-point STBC system is governed by the Frobenius norm of the associated $n \times m$ channel matrix $\mathbf{H}$. For $m \geq 1$, the post-processing received SNR is proportional to $\frac{\zeta_m}{m}\|\mathbf{H}\|_F^2 r^{-\eta}$, where $\zeta_m = 1$ if $m = 1, 2$ and $\zeta_m = 2$ otherwise. The factor of ζ_m/m arises from power normalization and the fact that the rate of a code derived from a GCOD is 1/2 for $m > 2$ [14].

Now we can apply the definition for $H(r)$ given by (5) by letting $X = \|\mathbf{H}\|_F^2 = \sum_{i,j} |h_{ij}|^2$, where h_{ij} is the complex coefficient modelling the transfer characteristics of the channel between the jth transmit antenna ($1 \leq j \leq m$) and the ith receive antenna ($1 \leq i \leq n$). Here, we make the fairly standard assumption that h_{ij} is a circularly symmetric complex Gaussian random variable with zero mean and unit variance. Consequently, X is chi-squared distributed with $2mn$ degrees of freedom, and its cumulative distribution function is given by $F_X(x) = \gamma(mn, x)/\Gamma(mn)$, where $\Gamma(\cdot)$ and $\gamma(\cdot,\cdot)$ are the standard and lower incomplete gamma functions, respectively.

We can now evaluate the connectivity mass (3) for the H function given by (5) and observe its behavior as m, n grow large. Using (6), M can be evaluated to yield

$$M_{\text{dc}} = \frac{\omega}{d}\left(\frac{\zeta_m}{m\beta}\right)^{\mathcal{C}} \frac{\Gamma(mn + \mathcal{C})}{\Gamma(mn)} \tag{9}$$

where we have used a "dc" subscript to indicate the relation to diversity coding. For large m and/or n, we can use the Stirling formula $\Gamma(x) \sim \sqrt{2\pi}\, x^{x+\frac{1}{2}} e^{-x}$ to obtain the scaling law

$$M_{\text{dc}} = \frac{\omega}{d}\left(\frac{\zeta_m n}{\beta}\right)^{\mathcal{C}} \left(1 + O\Big(\tfrac{1}{mn}\Big)\right), \quad m, n \to \infty. \tag{10}$$

[1]Note that the impact that boundaries have on connectivity can be observed from (3). Specifically, $M \propto \omega$, i.e., the ability of a given node to form a connection is proportional to the "visible region" that is available. Linear scaling in ω at a local level translates to exponential scaling in the global sense according to (1). See [13] for a rigorous treatment.

[2]We touch on mutual information outage in section III-B3.

The connectivity exponent $\mathcal{C}$ arises in the expression given above in a manner similar to the power scaling law. This reinforces our assertion that the ratio has special importance, and we surmise that a universality property exists for scaling of locally defined system parameters.

2) Beamforming: For MIMO-MRC transmissions, the received SNR (after MRC) is proportional to $\lambda_{\max}(\mathbf{H}'\mathbf{H})r^{-\eta}$, with $\lambda_{\max}(\cdot)$ denoting the maximum eigenvalue of the argument [15]. The behavior of $\lambda_{\max}$ in the limit of large m, n is required in order to make progress. Here, we can apply the following result due to Edelman [16, Lemma 4.3][3]:

Lemma 1: Let $x_n \xrightarrow{p} x$ signify that for all $\varepsilon > 0$, $\lim_{n\to\infty} P(|x - x_n| > \varepsilon) = 0$. Now, suppose the $n \times m$ matrix $\mathbf{H}$ has independent circularly symmetric complex Gaussian entries, each with zero mean and unit variance. Then $\mathbf{W} = \mathbf{H}'\mathbf{H}$ has a complex Wishart distribution and

$$(1/n)\lambda_{\max}(\mathbf{W}) \xrightarrow{p} (1+\sqrt{y})^2, \qquad \text{for } \frac{m}{n} \to y,\ 0 \le y < \infty. \tag{11}$$

For the definition of H given in (5), we draw inspiration from this lemma and write

$$H(r) \approx \begin{cases} 1, & r < \left(\frac{(1+\sqrt{y})^2 n}{\beta}\right)^{\frac{1}{\eta}} \\ 0, & \text{otherwise} \end{cases} \tag{12}$$

for large n. Consequently, letting $\mu(n) = (1+\sqrt{y})^2 n$, we are motivated to write

$$\frac{M_{\mathrm{b}}}{\omega} = \int_0^{(\frac{\mu}{\beta})^{\frac{1}{\eta}}} r^{d-1}\,\mathrm{d}r + \epsilon(n) = \frac{1}{d}\left(\frac{(1+\sqrt{y})^2 n}{\beta}\right)^{\mathcal{C}} + \epsilon(n) \tag{13}$$

where a "b" subscript is used to indicate the relation to beamforming. The error term is given by

$$\epsilon(n) = \underbrace{\int_{(\frac{\mu}{\beta})^{\frac{1}{\eta}}}^{\infty} r^{d-1} H(r)\,\mathrm{d}r}_{\epsilon_+(n)} - \underbrace{\int_0^{(\frac{\mu}{\beta})^{\frac{1}{\eta}}} r^{d-1}(1-H(r))\,\mathrm{d}r}_{\epsilon_-(n)} \tag{14}$$

which increases like[4] $O(n^{\mathcal{C}-\frac{2}{3}})$. Thus, we have

$$M_{\mathrm{b}} = \frac{\omega}{d}\left(\frac{(1+\sqrt{y})^2 n}{\beta}\right)^{\mathcal{C}} \left(1 + O\left(n^{-\frac{2}{3}}\right)\right), \qquad m, n \to \infty,\ \frac{m}{n} \to y. \tag{15}$$

3) Comparison of the Two Multi-Antenna Schemes: Let us compare (10) and (15). Suppose the number of transmit antennas per node is fixed at $m = 2$, in which case $\zeta_m = 1$ and $y = 0$, and thus the leading order of M_{dc} is the same as that of M_{b}. However, we see that the first-order corrections for the two observables differ. This is illustrated in Fig. 1, where exact results for the connectivity masses of the two systems are presented along with leading-order terms as a function of n. In the figure, the solid lines show the leading-order behavior, while the marker data was obtained from the direct calculation of (9) in the case of diversity coding and by numerically calculating (6) for beamforming. The solid angle ω and the proportionality constant β were set equal to $\pi/4$ and 1, respectively; however, the general conclusions drawn here are independent of particular values of ω and β.

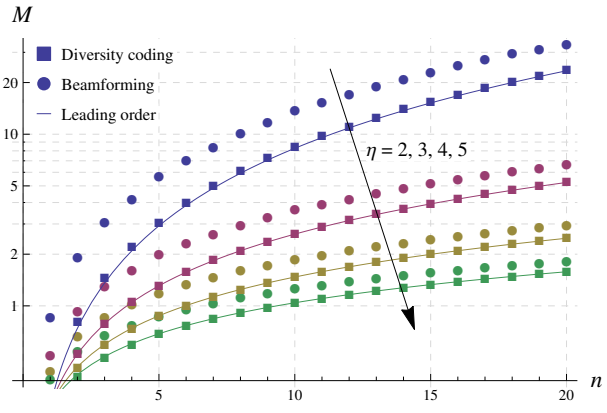

Fig. 1. Connectivity mass vs. n for $m = 2$, $d = 3$, and various values of η, corresponding to connectivity exponents $\mathcal{C} = \frac{3}{2}, 1, \frac{3}{4}, \frac{3}{5}$. The solid lines correspond to the leading-order term given in (15) (equivalently (10)), whereas the data represented by markers was obtained from (9) for the diversity coding scenario and by numerically calculating (6) for the beamforming case.

Three observations can be made from this example. The first is that the difference in first-order corrections is apparent, and beamforming actually provides a benefit over diversity coding for finite numbers of receive antennas. Yet, convergence to the leading order can be seen for both schemes. The second observation is that the leading-order expression well approximates the exact connectivity mass, even for small numbers of antennas. For STBC, the approximation is very accurate. The third observation is that the derivative of the connectivity mass satisfies $M'(n) \propto n^{\mathcal{C}-1}$. Indeed, we can deduce from the figure that progressive improvements are obtained for $\mathcal{C} > 1$ and diminishing returns are experienced for $\mathcal{C} < 1$.

For any other fixed m greater than two, $M_{\mathrm{dc}} > M_{\mathrm{b}}$ to leading order by a factor of $2^{\mathcal{C}}$. However, STBC suffers from a lower rate than MIMO-MRC in this case. Consequently, it is informative to consider a modified view of the connectivity mass based on pairwise mutual information outage. This can be easily achieved by redefining H_{ij} in (4) to be

$$H_{ij}(r) = P\left(\frac{1}{\zeta_m}\log_2(1 + \mathsf{SNR}(r)\cdot X_{ij}) > R\right) \tag{16}$$

where R is a target rate threshold and $\zeta_m = 1$ if STBC is employed and $m \le 2$ or if MIMO-MRC is considered, and $\zeta_m = 2$ otherwise. By rearranging to obtain the form given in (4), it is clear that $\mathsf{SNR}_{th} = 2^{\zeta_m R} - 1$, and all subsequent calculations follow accordingly, but with β replaced by $\beta(2^{\zeta_m R} - 1)$ to explicitly account for the difference in rate characterised by ζ_m. Thus, we deduce from (10) and (15) that $M_{\mathrm{dc}} < M_{\mathrm{b}}$ since $(2^{2R} - 1) > 2(2^R - 1)$ for $R > 0$.

Now, let m and n scale such that their ratio approaches $y > 0$, then the relation $M_{\mathrm{dc}} < M_{\mathrm{b}}$ is maintained when considering

[3]Edelman's result assumed the complex Gaussian entries of $\mathbf{H}$ had unit variance *per dimension*, whereas the result we use here is for the case where each entry has unit variance *in total*, and thus this lemma is slightly different from that found in [16].

[4]The proof of this statement is omitted due to space restrictions.

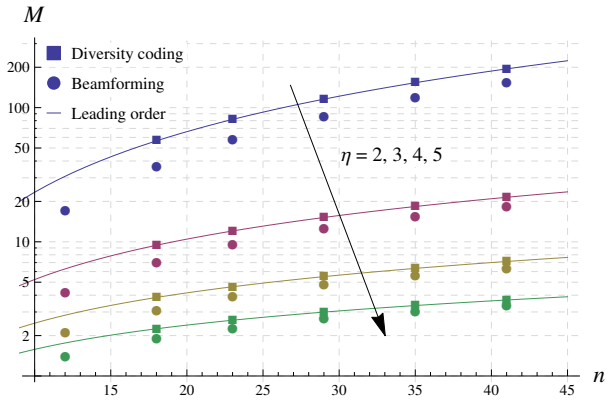

Fig. 2. Connectivity mass vs. n for $m \approx y_c n$, $d = 3$, and various values of η, corresponding to connectivity exponents $\mathcal{C} = \frac{3}{2}, 1, \frac{3}{4}, \frac{3}{5}$. The solid lines correspond to the leading-order term given in (15) (equivalently (10)), whereas the data represented by markers was obtained from (9) for the diversity coding scenario and by numerically calculating (6) for the beamforming case.

mutual information outage. But neglecting the rate differences and focusing only on SNR outage (a proxy for reliability in delay-tolerant networks) vis-à-vis (4), we see that when $y = (\sqrt{2}-1)^2 \approx 0.172$ the leading orders of the two schemes are equal. Denote this critical value y_c. For $y < y_c$, diversity coding is favored over beamforming to leading order, with the opposite being true for $y > y_c$. Again, we must be careful for finite n since the correction terms differ. To draw further conclusions, we have plotted the connectivity mass against n with $y \approx 0.172$ in Fig. 2. The markers shown in the figure correspond to the (m, n) pairs $(2, 12)$, $(3, 18)$, etc., noting that we have not plotted the points corresponding to $m = 2$ for the STBC scheme since the leading-order behavior differs for the two schemes in this case. We see from Fig. 2 that diversity coding is preferred over beamforming for small n. It is worth noting that although the numbers of antennas considered here are large in the conventional sense, new networking paradigms such as large-scale antenna systems and nano networks suggest that such an eventuality is not beyond the realms of possibility.

IV. Conclusions and Design Implications

In this paper, we studied how scaling the per-node transmit power and the number of antennas affects network connectivity. We defined the *connectivity exponent*, $\mathcal{C}$, to be the ratio of the dimension of the network domain to the path loss exponent, and showed that local connectivity scales like $O(z^{\mathcal{C}})$ in several parameters of interest, pointing to a universality property in random geometric network analysis. Our theory was validated with simulations, and it was shown that the derived scaling laws act as good approximations in finite systems.

The scaling laws developed herein can be exploited to mitigate the deleterious effects that boundaries present in confined networks. For example, in the case of transmit power scaling, we can use this analysis to deduce that, for some nominal transmit power P_{T_0} that defines the target connectivity probability of a homogeneous network, we must choose P_T for the bounded network to satisfy

$$P_T = (\Omega/\omega)^{1/\mathcal{C}} P_{T_0}. \tag{17}$$

Similar results hold if we wish to mitigate boundary effects using multiple antennas. Let our reference point be given by the connectivity mass corresponding to a homogeneous network connected by single-input single-output pairwise links, which can be computed to be $\Omega\Gamma(1+\mathcal{C})/(\beta^{\mathcal{C}} d)$ using (9). In a bounded network, we can focus on a particular feature of solid angle ω and use, for example, (15) to obtain the antenna scaling law that will ensure the effect that this feature has on local connectivity is mitigated. Specifically, we see that

$$wn \approx \left(\tfrac{\Omega}{\omega}\Gamma(1+\mathcal{C})\right)^{1/\mathcal{C}} \tag{18}$$

where $w = \zeta_m$ for diversity coding and $w = (1+\sqrt{y})^2$ for beamforming. This simple discussion hints at the possibility of designing more sophisticated network optimisation methods based on the framework presented here.

Acknowledgment

This work was undertaken within the FP7 DIWINE project (Grant Agreement CNET-ICT-318177).

References

[1] S. C. Ng, W. Zhang, Y. Zhang, Y. Yang, and G. Mao, "Analysis of access and connectivity probabilities in vehicular relay networks," *IEEE J. Sel. Areas Commun.*, vol. 29, no. 1, pp. 140–150, 2011.

[2] Z. Khalid, S. Durrani, and J. Guo, "A tractable framework for exact probability of node isolation and minimum node degree distribution in finite multihop networks," *IEEE Trans. Veh. Technol.*, vol. 63, no. 6, pp. 2836–2847, 2014.

[3] V. Ravelomanana, "Extremal properties of three-dimensional sensor networks with applications," *IEEE Trans. Mobile Computing*, vol. 3, no. 3, pp. 246–257, 2004.

[4] G. Mao and B. Anderson, "Towards a better understanding of large scale network models," *IEEE/ACM Trans. Netw.*, vol. 20, no. 2, pp. 408–421, Apr. 2012.

[5] P. Gupta and P. Kumar, "Critical power for asymptotic connectivity," in *Decision and Control, 1998. Proceedings of the 37th IEEE Conference on*, vol. 1. IEEE, 1998, pp. 1106–1110.

[6] F. Xue and P. Kumar, "The number of neighbors needed for connectivity of wireless networks," *Wireless networks*, vol. 10, no. 2, pp. 169–181, 2004.

[7] ——, "On the θ-coverage and connectivity of large random networks," *IEEE Trans. Inf. Theory*, vol. 52, no. 6, pp. 2289 –2299, Jun. 2006.

[8] W. Jia and J. Wang, "Analysis of connectivity for sensor networks using geometrical probability," *IEE Proc.-Commun.*, vol. 153, no. 2, pp. 305–312, Apr. 2006.

[9] Z. Khalid and S. Durrani, "Connectivity of three dimensional wireless sensor networks using geometrical probability," in *Communications Theory Workshop (AusCTW), 2013 Australian*. IEEE, 2013, pp. 47–51.

[10] R. Rajagopalan and P. Varshney, "Connectivity analysis of wireless sensor networks with regular topologies in the presence of channel fading," *IEEE Trans. Wireless Commun.*, vol. 8, no. 7, pp. 3475–3483, Jul. 2009.

[11] J. P. Coon, O. Georgiou, and C. P. Dettmann, "Full connectivity: corners, edges and faces," *Journal of Statistical Physics*, vol. 147, no. 4, pp. 758–778, 2012.

[12] O. Georgiou, C. Dettmann, and J. P. Coon, "Connectivity of confined 3D networks with anisotropically radiating nodes," *IEEE Trans. Wireless Commun.*, vol. 13, no. 8, pp. 4534–4546, 2014.

[13] M. D. Penrose, "Connectivity of soft random geometric graphs," *Annals of Applied Probability (accepted), available on arXiv (arXiv:1311.3897v2)*, 2015.

[14] V. Tarokh, H. Jafarkhani, and A. R. Calderbank, "Space-time block codes from orthogonal designs," *IEEE Trans. Inf. Theory*, vol. 45, no. 5, pp. 1456–1467, 1999.

[15] M. Kang and M. Alouini, "Largest eigenvalue of complex Wishart matrices and performance analysis of MIMO MRC systems," *IEEE J. Sel. Areas Commun.*, vol. 21, no. 3, pp. 418–426, Apr. 2003.

[16] A. Edelman, "Eigenvalues and condition numbers of random matrices," *SIAM Journal on Matrix Analysis and Applications*, vol. 9, no. 4, pp. 543–560, 1988.